Steering Acoustically Propelled Nanowire Motors towards Cells in a Biologically Compatible Environment using Magnetic Fields

*Suzanne Ahmed,[1] Wei Wang,[1] Lamar O. Mair,[6,6b] Robert D. Fraleigh,[2] Sixing Li,[3,5] Luz Angelica Castro,[7] Mauricio Hoyos,[7] Tony Jun Huang,[4] and Thomas E. Mallouk[1,3]**

Departments of [1]Chemistry, [2]Physics, [3]Biochemistry and Molecular Biology, [4]Engineering Science and Mechanics, and [5]Cell and Developmental Biology Graduate Program, The Pennsylvania State University, University Park, PA 16802 USA

[6] Center for Nanoscale Science and Technology, National Institute of Standard and Technology, 100 Bureau Drive, Stop 6200, Gaithersburg, MD 20899 USA

[6b]Maryland Nanocenter, University of Maryland, College Park, MD 20742 USA

[7]Laboratoire de Physique et Mécanique des Milieux Hétérogènes,UMR7636 CNRS, UMPC, ESPCI,10 rue Vauquelin, 75005 Paris, France

ABSTRACT: The recent discovery of fuel-free propulsion of nanomotors using acoustic energy has provided a new avenue for using nanomotors in biocompatible media. Crucial to the application of nanomotors in biosensing and biomedical applications is the ability to remotely control and steer them towards targets of interest such as specific cells and tissues. We demonstrate *in vitro* magnetic steering of acoustically powered nanorod motors in a biologically compatible environment. Steering was accomplished by incorporating (40 ± 5) nm thick nickel stripes into the electrochemically grown nanowires. An external magnetic field of 15 mT to 40 mT was used to orient the motors, which were acoustically propelled along their long axes. In the absence of a magnetic field, (300 ± 30) nm diameter, (4.3 ± 0.2) μm long nanowires with (40 ± 5) nm thick magnetic stripes exhibit the same self-acoustophoretic behavior, including pattern formation into concentric nanowire circles, aligned spinning chains and autonomous axial motion, as their non-magnetic counterparts. In a magnetic field these wires and their paths are oriented as evidenced by their comparatively linear trajectories. Coordinated motion of multiple motors and targeting of individual motors towards HeLa cells with micron-level precision was demonstrated (End of Abstract).

Research into the propulsion and control of nano- and microscale motors has grown steadily over the past decade. [1-10] Research in this field has been largely driven by potential applications in biosensing and biomedicine.[11-16] The recent discovery of the propulsion of nanomotors using acoustic energy has provided a new avenue to the use of nanomotors in biocompatible media.[17-18] Self-acoustophoretic nanowire motors are especially attractive as they are fuel-free and hence allow continuous propulsion that is not limited by the supply of fuel. They are operated in a frequency and power range that is biologically safe.[17,19-20] The power density used in these experiments is (13 ± 1) mW/cm^2 which is well below the FDA limit of 740 mW/cm^2 for diagnostic ultrasound.[19-20] The self-acoustophoretic mechanism also allows one to change the nanomotor speed easily by adjusting the applied power.[21-26] In order to take full advantage of ultrasonically propelled motors one must be able to direct and guide their motion towards targets of interest such as cells and tissues. Here we demonstrate that remote steering and targeting of acoustically powered motors is possible by using externally applied magnetic fields. As in previous reports of magnetically oriented autonomous nanomotors, a magnetic segment was incorporated into the nanowires.[27-29] A ferromagnetic nickel stripe was electrochemically grown between diamagnetic Au and Ru segments, as shown in Figure 1, and it responded to a weak external magnetic field that could be oriented to define the motor's path in two dimensions.

It should be noted that uncertainties in these measurements derive primarily from experiment to experiment distributions. Measurement error for each of the measured values was less than 5 % of the reported uncertainty, and all representations of uncertainty are given as one standard deviation.

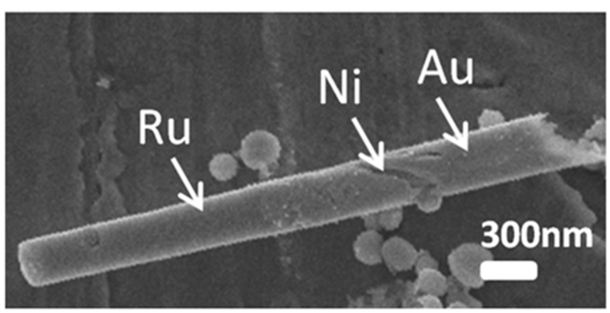

Figure 1. A representative FE-SEM image of the Au-Ni-Ru nanowire motors.

Behavior of Nanomotors in Static Magnetic Fields. When excited by ultrasonic standing waves near the resonant frequency of the cylindrical cell (3.77 ± 0.01 MHz), nanowires with (40

± 5) nm thick magnetic stripes exhibited the same behavior as their non-magnetic counterparts, including levitation to the midpoint of the cell, pattern formation into concentric nanowire circles, alignment into spinning chains, and autonomous axial motion.[17] The polar alignment of Au-Ni-Ru wires in spinning chains at the acoustic nodal lines, with the ruthenium ends leading, was also consistent earlier observations with non-magnetic Au-Ru nanorods. The average speed of the wires did not change with application of a static magnetic field: speeds of (26 ± 12) μm/s and (26 ± 18) μm/s were observed, without and with the field, respectively (the resulting Reynolds number is approximately $(1 \pm 0.8) \times 10^{-4}$). These values are based on 46 measurements of wires with an applied magnetic field and 120 measurements of wires with no applied field. The positional measurement error was less than 0.3 μm and thus the distribution in speed derives primarily from wire to wire speed variation. However, the pattern of movement changed markedly, as shown in Figure 2. In the absence of magnetic field, wire trajectories followed loops (possibly from slight bending of the wires, asymmetry in the wire end shape, and/or localized acoustic streaming) and also contained random turns, but in the magnetic field they followed straight line trajectories. In the static field (applied parallel to the y axis in Figure 2) the majority of the wires align with their long axis oriented perpendicular to the applied field (along the x axis in Figure 2). The range of angles observed between the direction of movement and the applied field can be explained by the fact that the Ni stripes in the wires in general were not perfectly perpendicular to the wire axis (Figure 1). These static field experiments were conducted at a constant field of (40 ± 1) mT by placing a NdFeB magnet (6.60 ± 0.03) cm from the active area of the acoustic cell.

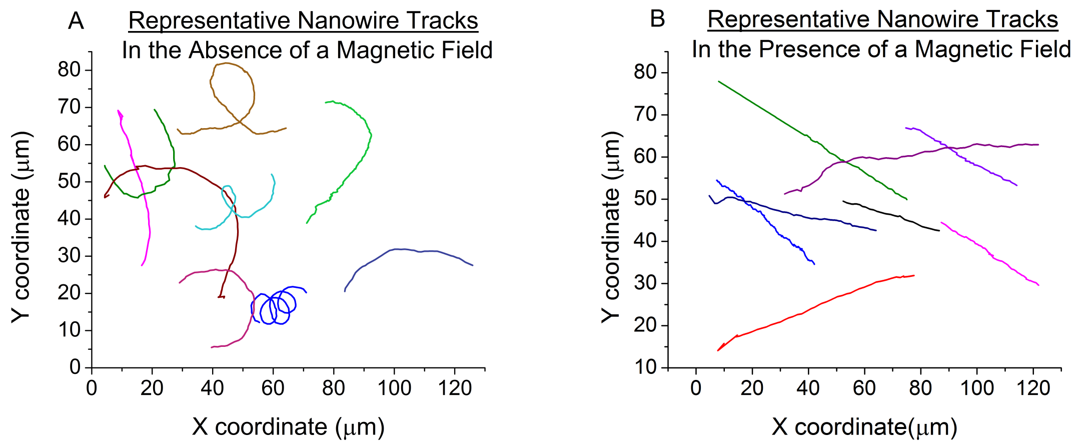

Figure 2. Representative nanowire tracks plotted from the x and y coordinates obtained from tracking nanowires, the bottom left of the screen is defined as the origin. (A) Representative tracks in the absence and (B) in the presence of a magnetic field; field direction is indicated by the arrow.

on the nanowires within the cell as calculated from equation (1):

(1)

is the magnetic dipole moment of the wire $(6.5 \pm 0.5) \times 10^{-15}$ A$\cdot$ m^2 as determined by ensemble superconductong quantum interference device (SQUID) magnetometry measurements (Figure 3), is the field strength of the aligning magnet. From this value, the energy required to turn the nanowire through 90° (i.e., to align the long axis parallel to the field) is approximately 2×10^{-16} J, which is much greater than the thermal energy $k_BT \approx 4 \times 10^{-21}$ J.

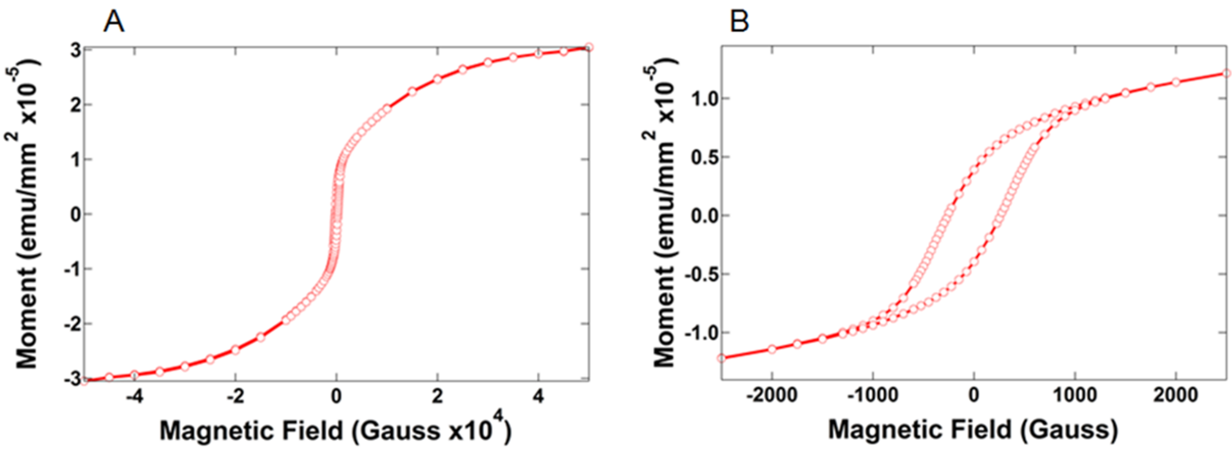

Figure 3. SQUID magnetometry measurements. (a) Magnetization of a Au-Ni-Ru nanowire sample from -5 to 5T showing the saturation magnetization used to calculate the magnetic dipole moment of the wires. (b) Zoomed in hysteresis curve from -2500G to 2500G showing the ferromagnetic character of the nanowire sample.

In the low Reynolds number limit, the acoustic propulsion force on the wires is equal to the drag force experienced by the wires. The axial propulsion force on the wires from scattering of ultrasonic waves was determined from the Stokes drag equation (2) to be (0.26 ± 0.05) pN for wires traveling at 25 μm/s.

$$F_{drag} = 2\pi\eta Lv \,/\, [\ln(L/R) - 0.72] \tag{2}$$

where η is the dynamic viscosity of water at 293 K, L is the length of the wire, R is its radius, and v is its velocity.[29] In contrast, the axial propulsion force on the nanowires due to the magnetic field was negligible as evidenced by the fact that there is no change in the speed of the wires before and after the application of the field. This is to be expected as the magnetic field was essentially uniform over the 100 μm to 200 μm length scale under view.[27]

Magnetic Steering. Using handheld magnets at a distance of 1 cm to 1.5 cm, which apply a (15 ± 1) mT to (30 ± 1) mT field at the sample location, it was possible to reversibly disrupt patterns, such as spinning chains that are formed in the acoustic field, by reorienting the wires perpendicular to the chain. The applied field could also steer autonomously moving wires that were traveling as fast (170 ± 10) μm/s. The disruption of pattern formation can be seen in Figure 3 and Video S1 in Supporting Information.

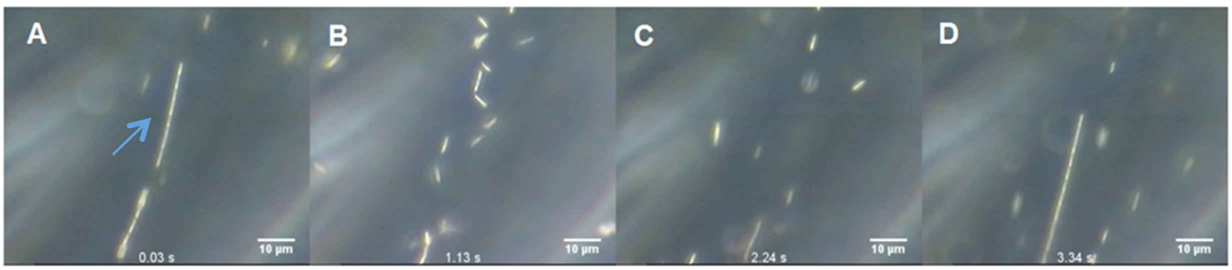

Figure 4. (a) Nanowire motors within an acoustic cell assemble at nodal lines, eventually forming patterns such as spinning chains. (b) Upon the application of an oscillating magnetic field the chain is rapidly disrupted and the nanowire motors follow varying trajectories not confined to the nodal lines. (c, d) Upon the removal of the field the chain re-organizes. Times of frames (a-d) are indicated. (Video S1 in Supporting Information).

Magnetic steering was demonstrated with nanowire motors moving at axial speeds ranging from (8 ± 3) μm/s to (170 ± 10) μm/s. This is illustrated by the ensemble motion of wires, which could be directed to move in concert as shown in Fig. 4. The autonomous nature of the acoustically propelled motion was retained when the magnetic field was applied. The top panel of Fig. 4 illustrates the magnetic steering of groups of motors that were initially traveling in approximately the same direction and then taken through a series of turns by re-orienting the external field. The bottom panel of Figure 4 shows the effect of the field on wires traveling in opposite directions. These wires are also re-oriented in the field, but in opposite directions, and were also made to take multiple sharp U-turns.

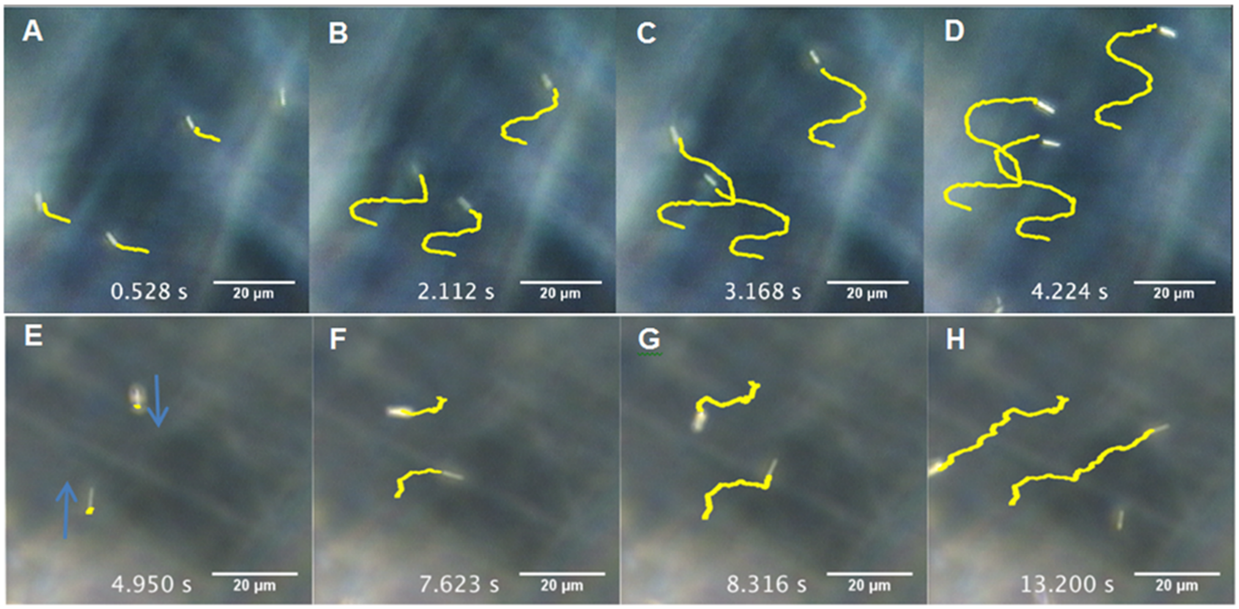

Figure 5. Top panel: Steered ensemble motion of wires moving at (25 ± 5) μm/s, showing (a) earlier and (b) later times in the trajectory. Yellow tracking lines are superimposed on the final frame of the video. The wires undergo multiple guided U-turns (Videos S2 and S3 in Supporting Information). Times of frames (a-d) are indicated. **Bottom panel:** Autonomous steering of motors moving at (8 ± 3) μm/s. Times of frames (e-h) are indicated and arrows show initial direction of motion in (e) and consequent guided sharp U-turns (f-h). (Video S4 in Supporting Information).

Cell Targeting Experiments. For possible bioanalytical and biomedical applications, it is important to show that acoustically powered nanomotors can be steered in a biocompatible environment. Here we demonstrate the magnetic steering of nanomotors towards live HeLa cells in an aqueous phosphate buffer. Nanomotors were mixed with HeLa cells and placed into the acoustic cell. Cell viability tests showed no significant degradation after 20 min exposure to acoustic excitation at the power levels used in the steering experiments (see Supporting Information). In Video S5 (see Supporting Information) one nanomotor was selected and guided towards a cell. At the start of the video (Video S5), in order to demonstrate directional control, the wire was taken through multiple 180º turns before guiding it towards the targeted cell. It was possible to steer nanowire motors towards cells that were adjacent in aggregates and hence only microns apart. Targeting of a single nanowire towards an individual cell, and an approximately 90º turn of a group of nanowires into a group of cells, are illustrated in Figure 5. Nanowire targeting toward cells was successfully repeated multiple times to ensure the robustness of the technique.

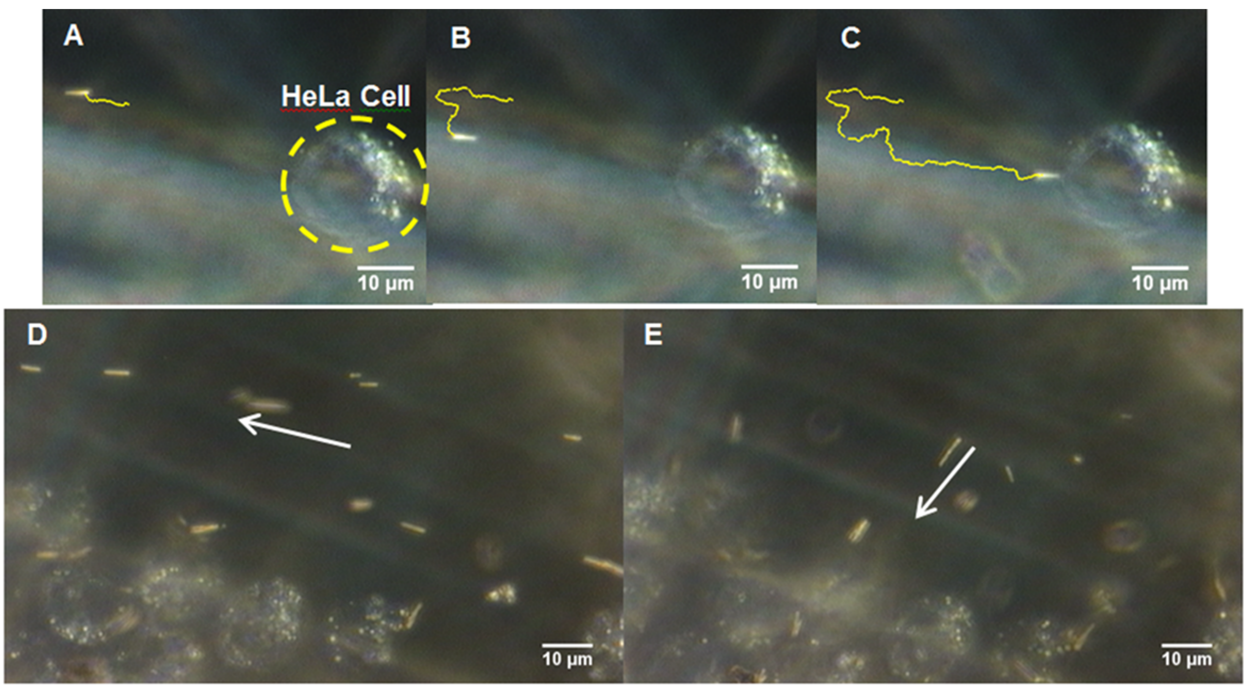

Figure 6. **Top panel**: (a-c) Nanomotor targeting towards a HeLa cell. Nanowires were guided to make multiple U-turns to demonstrate control before being steered towards the live cell. (see Video S5 of Supporting Information). **Bottom panel**: (d) Nanowires are moving parallel to a group of cells, with their direction indicated by the arrow. (e) By turning the external field,

nanowires are magnetically steered through an approximately 90° turn towards the cells. (Video S6 of Supporting Information)

These experiments have demonstrated that it is possible to suppress random motion and exert relatively fine control over the steering of acoustically propelled nanomotors using a weak external magnetic field. Both the propulsion and steering of these motors can be carried out in biocompatible buffers, as evidenced by steering of motors towards live cells in these media.

Methods. *Nanowire growth and characterization.* Bimetallic and trimetallic nanowires were grown electrochemically using commercial anodic aluminum oxide (AAO) membranes (Whatman Inc., nominal pore diameter 200 nm) as templates. Segmented gold-nickel-ruthenium wires were made by sequentially changing the plating solution within an electrochemical cell. A two-electrode electrochemical cell was used for the plating of silver, nickel and gold.[31] A silver layer evaporated onto the AAO membrane served as the cathode and a platinum wire as the anode. Ruthenium was plated in a three electrode cell with an additional Ag/AgCl electrode serving as the reference electrode. A thin gold adhesion layer was deposited between the nickel and ruthenium segments to prevent nanowire fragmentation during release. Gold and ruthenium deposition was conducted under conditions identical to those used previously in order to yield wires with similar morphological and shape asymmetry.[17] Nickel was deposited at a constant current density of 0.7 mA/cm^2 for 3 min.

The lengths of the nickel segments were (40 ± 5) nm, smaller than a single magnetic domain which is typically ≈150 nm, and also smaller than the diameter of the nanorod. This ensured that the easy axis and hence the direction of magnetization was approximately perpendicular to the nanowire long axis.[27,32-33] In this arrangement the motors can be steered with a magnetic field in the plane of the acoustic cell; the field applies substantial torque but minimal axial force to the nanowire. In the static field experiments described above, the majority of the wires align with their long axis oriented perpendicularly (along the x axis in Figure 2) to the applied field (the y axis direction in Figure 2).

The magnetic properties of the nanowires were characterized using SQUID magnetometry. The magnetic susceptibility of a 7 mm^2 portion of the template with embedded wires was measured at 5 K from 5 T to -5 T. A background measurement of a control sample containing gold-ruthenium wires grown under identical conditions, but without the nickel segment, was made for subtraction from the sample measurement. The magnetic dipole moment per wire (μ) was determined by dividing the total saturation magnetization of the sample by the number of wires contained within it and was determined to be approximately $(6.5 \pm 0.5) \times 10^{-15}$ $A \cdot m^2$. This value was used to determine the torque on the wires in the applied magnetic fields (Eqn. 1).

Acoustic propulsion experiments. The cylindrical acoustic cell with a height of (180 ± 10) μm and a diameter of (5.0 ± 0.1) mm has been described in an earlier work, and was used in all experiments.[17] The solution in the cell was excited by a piezoelectric disc transducer (1 mm thick) affixed to the center of a stainless steel plate (4.2 cm × 4.2 cm × 1 mm). Kapton tape was applied to the opposite side of the steel plate, and a hole punched in the center of the tape defined the cell. A glass microscope cover slip was placed on the cell during the experiments as a reflector to set up a standing wave. The resonant frequency of the cell center was (3.77 ± 0.01) MHz. Experiments were conducted on wires in the levitation plane at the midpoint of the cell at frequencies close to the resonance frequency. The voltage had a peak to peak value of 10 V and was applied using a waveform generator.

The behavior of the acoustically propelled nanowire motors in the presence of a static magnetic field was studied and compared to their behavior in the absence of a magnetic field. A cylindrical NbFeB magnet (2.50 ± 0.01) cm in diameter and (7.60 ± 0.01) cm in length was held in the plane of the cell at a fixed distance to maintain a constant field strength at the sample. The strength of the applied magnetic field was measured using a digital DC gaussmeter. The average speed for 46 and 120 wires was determined with the magnetic field on and off, respectively. For steering experiments, hand held magnets were used. The external magnetic field was applied using six rectangular FeNbB magnets (2.5 cm × 2.5 cm × 0.625 cm) in the plane of the cell, at a distance of 1 cm to 1.5 cm from the wires. The strength of the applied magnetic field was measured using a digital DC gaussmeter.

Nanowire motion was tracked using the open access program Video Spot Tracker (http://cismm.cs.unc.edu/downloads/?dl_cat=3) both in the presence and absence of a magnetic field. Videos of nanomotor motion were taken at 500 × magnification at a frame rate of 30 s^{-1}.

For cell targeting experiments, living human cervical cancer cells (HeLa cells) were used. The cells were used within one day of culture and stored refrigerated in a phosphate buffer solution that is 0.1 M phosphate, 0.15 M NaCl at a pH of 7.2. Details of cell growth and cell viability tests can be found in Supporting Information.

Acknowledgments

We thank Prof. Nitin Samarth for helpful discussions and for use of the SQUID magnetometer. This work was supported by the National Science Foundation under MRSEC grant DMR-0802404. Analytical instrumentation used in this work was supported by the Pennsylvania State University Materials Research Institute Nanofabrication Laboratory under National Science

Foundation Cooperative Agreement No. ECS-0335765. The tracking software Video Spot Tracker was developed at the CISMM at the University of North Carolina at Chapel Hill, supported by the NIH NIBIB (NIH 5-P41-RR02170). LOM acknowledges support under the Cooperative Research Agreement between the University of Maryland and the National Institute of Standards and Technology Center for Nanoscale Science and Technology, Award 70ANB10H193, through the University of Maryland.

Supporting Information

Videos illustrating acoustic propulsion and magnetic steering, a description of the cell viability test, and cell viability data. This material is available free of charge via the Internet at http://pubs.acs.org.

Corresponding Author

*Email: tem5@psu.edu

Notes

The authors declare no competing financial interests.

Disclaimer

Certain commercial equipment, instruments, or materials are identified in this paper to foster understanding. Such identification does not imply recommendation or endorsement by the National Institute of Standards and Technology, nor does it imply that the materials or equipment identified are necessarily the best available for the purpose.

References

(1) Mallouk, T.; Sen, A. Powering Nanorobots. Scientific American 2009, 300, 72–77.

(2) Ozin, G. A.; Manners, I.; Fournier-Bidoz, S.; Arsenault, A., Dream Nanomachines. Adv. Mater. 2005, 17, 3011-3018.

(3) Fournier-Bidoz, S.; Arsenault, A. C.; Manners, I.; Ozin, G. A., Synthetic self-propelled nanorotors. Chem. Commun. 2005, 441-443.

(4) Mirkovic, T.; Zacharia, N. S.; Scholes, G. D.; Ozin, G. A., Nanolocomotion - Catalytic Nanomotors and Nanorotors. Small 2010, 6 (2), 159-167.

(5) Gibbs, J. G.; Zhao, Y. P., Design and characterization of rotational multicomponent catalytic nanomotors. Small 2009, 5 (20), 2304-8.

(6) Gibbs, J.; Zhao, Y., Catalytic nanomotors: fabrication, mechanism, and applications. Frontiers of Materials Science 2011, 5 (1), 25-39.

(7) Sengupta, S.; Ibele, M. E.; Sen, A., Fantastic Voyage: Designing Self-Powered Nanorobots. Angew Chem Int Edit 2012, 51, 8434-8445.

(8) Fischer, P.; Ghosh, A., Magnetically actuated propulsion at low Reynolds numbers: towards nanoscale control. Nanoscale 2011, 3, 557-563.

(9) Agarwal, A. ; Hess ,H. , Molecular motors as components of future medical devices and engineered materials", Journal of Nanotechnology in Engineering and Medicine 2009,1(1),011005.

(10) Wang, J.; Manesh, K. M., Motion control at the nanoscale. Small 2010, 6, 338-345.

(11) Hess, H. ; Jaeger, L., Nanobiotechnology. Current Opinion in Biotechnology 2010, 21,373-375.

(12) Qin, L. D.; Banholzer, M. J.; Xu, X. Y.; Huang, L.; Mirkin, C. A., Rational design and synthesis of catalytically driven nanorotors. J. Am. Chem. Soc. 2007, 129, 14870-14871.

(13) Nelson, B. J.; Kaliakatsos, I. K.; Abbott, J. J., Microrobots for Minimally Invasive Medicine. Annual Review of Biomedical Engineering 2010, 12, 55-85.

(14) Solovev, A. A.; Xi, W.; Gracias, D. H.; Harazim, S. M.; Deneke, C.; Sanchez, S.; Schmidt, O. G., Self-Propelled Nanotools. ACS Nano 2012, 6 (2), 1751-1756.

(15) Sanchez, S.; Pumera, M., Nanorobots: the ultimate wireless self-propelled sensing and actuating devices. Chem Asian J 2009, 4, 1402-10.

(16) Wang, J.; Gao, W., Nano/Microscale Motors: Biomedical Opportunities and Challenges. ACS Nano 2012, 6, 5745-5751.

(17) Wang, W.; Castro, L. A.; Hoyos, M.; Mallouk, T. E. Autonomous Motion of Metallic Microrods Propelled by Ultrasound. ACS Nano 2012, 1-30.

(18) Kagan, D.; Benchimol, M. J.; Claussen, J. C.; Chuluun-Erdene, E.; Esener, S.; Wang, J., Acoustic Droplet Vaporization and Propulsion of Perfluorocarbon-Loaded Microbullets for Targeted Tissue Penetration and Deformation. Angew Chem Int Edit 2012, 51, 7519-7522.

(19) Barnett, S. B.; Ter Haar, G. R.; Ziskin, M. C.; Rott, H.-D.; Duck, F. A.; Maeda, K., International recommendations and guidelines for the safe use of diagnostic ultrasound in medicine. Ultrasound in Medicine & Biology 2000, 26 (3), 355-366.

(20) Wang, W. Understanding the propulsion and assembly of autonomous nano- and micromotors powered by chemical gradients and ultrasound. Ph.D. thesis. The Pennsylvania State University 2013.

(21) Bruus, H. Acoustofluidics 7: The acoustic radiation force on small particles. Lab Chip 2012, 12, 1578-86.

(22) Lenshof, A.; Magnusson, C.; Laurell, T., Acoustofluidics 8: Applications of acoustophoresis in continuous flow microsystems. Lab Chip 2012, 12, 1210-1223.

(23) Friend, J.; Yeo, L. Y., Microscale acoustofluidics: Microfluidics driven via acoustics and ultrasonics. Rev Mod Phys 2011, 83, 647-704.

(24) Ding, X. Y.; Lin, S. C. S.; Kiraly, B.; Yue, H. J.; Li, S. X.; Chiang, I. K.; Shi, J. J.; Benkovic, S. J.; Huang, T. J., On-chip manipulation of single microparticles, cells, and organisms using surface acoustic waves. P Natl Acad Sci USA 2012, 109, 11105-11109.

(25) Shi, J.; Ahmed, D.; Mao, X.; Lin, S.-C. S.; Lawit, A.; Huang, T. J., Acoustic tweezers: patterning cells and microparticles using standing surface acoustic waves (SSAW). Lab Chip 2009, 9 (20), 2890-2895.

(26) Chen, Y.; Ding, X.; Steven Lin, S.-C.; Yang, S.; Huang, P.-H.; Nama, N.; Zhao, Y.; Nawaz, A. A.; Guo, F.; Wang, W.; Gu, Y.; Mallouk, T. E.; Huang, T. J., Tunable Nanowire Patterning Using Standing Surface Acoustic Waves. ACS Nano 2013, 7 (4), 3306-3314.

(27) Kline, T. R.; Paxton, W. F.; Mallouk, T. E.; Sen, A., Catalytic nanomotors: remote-controlled autonomous movement of striped metallic nanorods. Angew Chem Int Ed Engl 2005, 44, 744-6.

(28) Solovev, A. A.; Sanchez, S.; Pumera, M.; Mei, Y. F.; Schmidt, O. G., Magnetic Control of Tubular Catalytic Microbots for the Transport, Assembly, and Delivery of Micro-objects. Adv. Funct. Mater. 2010, 20, 2430-2435.

(29) Garcia-Gradilla,V.; Orozco, J.; Sattayasamitsathit, S.; Soto,F.; Kuralay,F.; Pourazary, A.; Katzenberg, A.; Gao, W.; Shen, Y.; Wang, J. Fucntionalized Ultrasound-Propelled Magnetically Guided Nanomotors: Toward Practical Biomedical Applications. ACS Nano. (2013) ASAP DOI: 10.1021/nn403851v.

(30) Happel, J.; Brenner, H. Low Reynolds Number Hydrodynamics; Prentice Hall: Englewood Cliffs, NJ, 1965; eq 5-11.52.

(31) Kline, T. R.; Tian, M.; Wang, J.; Sen, A.; Chan, M. W. H.; Mallouk, T. E., Template-Grown Metal Nanowires. Inorg. Chem. 2006, 45, 7555-7565.

(32) Love, J. C.; Urbach, A. R.; Prentiss, M. G.; Whitesides, G. M. Three-dimensional self-assembly of metallic rods with submicron diameters using magnetic interactions. J. Am. Chem. Soc 2003, 125, 12696-7.

(33) Wei, M.S.; Chou, S.Y. Size effects on switching field of isolated and interactive arrays of nanoscale single-domain Ni bars fabricated using electron beam nanolithography. J. Appl. Phys. 1994,76,6679-6681.

TOC graphic